Curr Radiol Rep (2015) 3:12
DOI 10.1007/s40134-015-0091-2

An Update of Practical CT Adrenal Imaging: What Physicians Need to Know

Brinda Rao Korivi · Khaled M. Elsayes · Silvana Faria de Castro · Naveen Garg · Aliya Qayyum

Published online: 4 March 2015

Abstract Computed tomography (CT) is increasingly being utilized for patient care, with a subsequent increase in the detection of incidental adrenal masses. It is important for physicians to be familiar with the various current and investigational CT techniques used to image and characterize adrenal masses, including noncontrast CT, dual-energy CT, post-contrast imaging with percentage washout calculations, and investigational techniques including histogram, perfusion, and biphasic CT analyses. Once an incidental adrenal mass is detected, it is important to utilize current CT adrenal imaging techniques to characterize adrenal masses and differentiate the indolent adrenal masses that may be left alone from malignant and symptomatic masses that need timely medical or surgical management. Current CT imaging techniques can be utilized to differentiate benign adrenal masses from malignant counterparts. In this article, we describe the common CT features of benign adrenal masses, including hyperplasia, adenoma, pheochromocytoma, and myelolipoma. We also describe the common CT features of malignant adrenal masses, including metastases, and adrenal cortical carcinoma.

This article is part of the Topical Collection on *Abdominal CT-An Update on Applications and New Developments.*

B. R. Korivi (✉) · K. M. Elsayes · S. F. de Castro · N. Garg · A. Qayyum
Department of Diagnostic Radiology, Abdominal Imaging Section – Unit 1473, T. Boone Pickens Tower, The University of Texas MD Anderson Cancer Center, Houston, TX 77030, USA
e-mail: brrao@mdanderson.org

Present Address:
B. R. Korivi
1400 Pressler Street, FCT 15.6070, Houston, TX 77030, USA

Keywords Adrenal gland · Adrenal incidentaloma · Adrenal characterization · CT

Introduction

The increased utilization of computed tomography (CT) imaging has resulted in increased detection of incidental findings in patients, including adrenal lesions. Approximately 4 % of CT scans have incidentally discovered adrenal lesions [1–4]. Various imaging modalities can be used for evaluating the adrenal gland, including MRI, PET imaging, and CT. In this article, we discuss CT as the most frequently used modality for initial evaluation of adrenal masses owing to its high sensitivity and specificity widespread availability. In one study, solitary adrenal lesions greater than 1 cm were detected in 8.7 % of a selected group of patients older than 65 years [5]. It is therefore important to be familiar with the imaging features of adrenal lesions and to the imaging characteristics that may be helpful in distinguishing benign from malignant lesions. With the advancement of adrenal imaging techniques, imaging characterization of adrenal lesions readily and efficiently performed, and can reduce the need for additional clinical work-up. Only in a small fraction of cases is surgery indicated, since the majority of adrenal lesions are benign, and are either hormonally inactive or have low activity.

In this article, we review the various CT acquisition techniques of imaging adrenal lesions, including noncontrast CT, post-contrast attenuation measurements (including arterial, venous, and delayed imaging), absolute and relative washout measurements, dual-energy imaging, and histogram analysis. After discussion of various CT techniques, we describe CT features of commonly encountered adrenal lesions, including

adrenal hyperplasia, adenomas, myelolipoma, adrenal cortical carcinoma (ACC), and metastases.

CT Techniques for Imaging Adrenal Lesions

Noncontrast CT

The measurement of the unenhanced attenuation values of adrenal lesions is important in diagnosing lipid-rich adenomas. Typical scanning parameters for CT adrenal imaging include a slice thickness of 3–5 mm, range of 200–300 milliampere second (mAs), and 120 peak kilovoltage (kVp). If an adrenal mass measures less than 10 Hounsfield units (HU), it is characteristic of a lipid-rich adenoma, and no further work-up is required [3, 6].

Contrast-Enhanced CT

If an adrenal lesion measures >10 HU on noncontrast CT, post-contrast imaging after intravenous contrast administration in venous and delayed phases with calculation of absolute and relative enhancement washout values may be helpful. The washout calculation is the most widely utilized technique for evaluation of adrenal masses [7•, 8].

For the absolute contrast enhancement washout (ACEW), a noncontrast, 60 s post-contrast, and 10–15 min post-contrast delayed phases are obtained, in which approximately half the mass is included in the measurement field. The percentage of ACEW is calculated as: $[(\text{contrast-enhanced HU at 60 s} - \text{delayed contrast HU})/(\text{contrast-enhanced HU at 60 s} - \text{noncontrast HU})] \times 100$.In a study by Caoili, the ACEW with a 60 % washout threshold to distinguish adenomas from non-adenomas had a sensitivity of 98 % and a specificity of 92 %. The specificity increased to 97 % if adenomas were compared to metastases [9••].

Because ACEW measurements require a noncontrast HU measurement and are not always obtained in daily practice, relative contrast enhancement washout patterns (RCEW) can be obtained as an alternate measurement [10]. The percentage of RCEW is calculated as: $\%\text{RCEW} = [(\text{contrast-enhanced HU at 60 s} - \text{delayed contrast HU})/(\text{contrast-enhanced HU at 60 s})] \times 100$.Caoli reported utilizing 40 % as the threshold relative enhancement value for the differentiation of lipid-poor adenomas from non-adenomas, with a sensitivity of 82 % and the specificity of 92 % [11–15].

Dual-Energy CT

Noncontrast dual-energy CT has been utilized to differentiate adenomas from non-adenomas, using the principle that decomposition of material may be performed through differences of attenuation at different energy levels. The different levels of energy enable differentiation between tissues with the same attenuation values on routine CT. Dual-energy characterization is based on the principle that an adrenal lesion exhibits different attenuations at different voltage settings. In one study, 31 nodules were measured at 140 and 80 kVp. Adenomas exhibited a decrease in lesion attenuation due to intracellular lipid content at 80 kVp compared with 140 kVp, with 50 % sensitivity and 100 % specificity [11]. Because of the low sensitivity (50 %), this technique currently has limited use and is undergoing continued investigation.

Dual-energy imaging has been performed with IV contrast, utilizing the adrenal protocol. The protocol includes unenhanced images, early and delayed contrast-enhanced CT images at 1 and 15 min. In one study, 49 adrenal masses were studied utilizing 120 kVP noncontrast CT, and 80 and 140 kVp early and delayed post-contrast dual-energy CT [16]. Absolute percentage loss of enhancement was calculated. It was determined that adrenal protocol dual-energy using unenhanced CT and washout rate does help in diagnosis of all lipid-poor adenomas. The attenuation values on dual-energy unenhanced CT were overall higher than a noncontrast CT. Therefore, the dual-energy noncontrast CT and washout rate had a lower sensitivity than noncontrast CT for lipid-rich adenomas [16].

A less common, experimental CT protocol of adrenal imaging used to differentiate adenomas from non-adenomas is quadriphasic imaging. The quadriphasic protocol in one study included an unenhanced phase, arterial phase at 35 s, venous phase at 80 s, and a 5-min delayed phase [17]. Quadriphasic imaging is a relatively novel method that allows for a faster workflow because of its 5-min delayed scan instead of a 10- or 15-min delayed scan [18]. The study demonstrated that the most frequent peak enhancement for adrenal lesions was in the portal phase in 67 % of lesions (70/104), versus in the arterial scan in which the peak enhancement occurred in 20 % of lesions (21/104). The arterial and portal venous phases were not as useful in distinguishing adenomas from non-adenomas. However, the relative peak washout represented the best imaging parameter for distinguishing between the two. The accuracy of distinguishing adenomas from non-adenomas by quadriphasic imaging was 86.5 % in unenhanced scans, 90.1 % with relative peak washout calculations with a greater than 30 % threshold, and 85.7 % for absolute washout calculations [18]. Quadriphasic imaging remains an investigational method, and not commonly used because of the need for delayed imaging at 10 and 15 min in order to obtain washout calculations, despite the tendency to better characterize non-adenomas from adenomas, as described in a previous section above.

Biphasic CT is another less common technique used to differentiate adenomas from non-adenomas by utilizing a relative wash-in ratio. In a study by Foti, noncontrast, arterial, and portal phase images were obtained [17]. The relative percentage wash-in ratio of adrenal lesions from unenhanced to the portal venous phase was calculated as: relative percentage wash-in ratio = 100 × (PA − NA)/NA, in which PA was the lesion attenuation in HU measured from the portal venous phase scan and NA was the lesion attenuation on the unenhanced scan. Relative percentage wash-in ratio from the arterial phase to the portal venous phase was also calculated as follows: relative percentage wash-in ratio = 100 × (PA − AA)/AA, in which PA was the lesion attenuation in HU measured on the portal venous phase scan and AA was the lesion attenuation on the arterial phase scan. The study examined the difference in the relative percentage wash-in ratio in the arterial and portal venous phases. It was theorized that benign lesions theoretically have patent vessels that enable easy contrast passage. Therefore, they have fast wash-in and washout from the arterial to portal phases. On the other hand, malignant lesions exhibit higher resistance to contrast flow and slow wash-in and washout patterns, due to a high cellular density and densely packed vessels [17]. In terms of wash-in techniques, venous phase post-contrast imaging was demonstrated to be useful in distinguishing adenomas from pheochromocytomas, which exhibits overall higher enhancement values. A limitation of biphasic imaging is that, due to overlap in contrast enhancement patterns between adenomas and non-adenomas, the wash-in patterns are not always reliable [17].

Perfusion Analysis

Adrenal gland perfusion analysis is another less common investigational technique and is based on the premise that blood flow perfusion of adrenal masses of various histological types is evaluated using deconvolution algorithm-based CT perfusion software. The blood flow perfusion parameters of adenomas and non-adenomas are examined, including blood flow, blood volume, mean transit time, and permeability surface-area production, which reflect adrenal nodule angiogenesis. Surface-area production and blood volume parameters differ between adenomas and non-adenomas. Adenomas have a higher permeability surface-area production value than do non-adenomas. When the blood volume was 9.325 mL/min per 100 g ($P < 0.05$), adenomas had a sensitivity of 76.9 % and specificity of 73.2 % [19].

Histogram Analysis

The histogram analysis method is another uncommon, investigational CT technique for characterizing adrenal lesions, particularly adenomas. In this method, a cursor is placed over approximately two-thirds of an adrenal mass, not including areas of necrosis. The method measures the number of pixels with negative attenuation and is used to identify the negative pixels on enhanced and unenhanced scans. The individual attenuation characterizes approximately 91 % of adenomas. Some studies have demonstrated a need for a threshold of greater than 10 % negative attenuation pixels for a high specificity. Although the specificity is high (over 90 %), this analysis is not a useful supplement for contrast CT scans due to a low sensitivity of 12 %. Its results are also variable based on the scanner and scanning technique used [20–24].

Commonly Encountered Adrenal Lesions

The normal adrenal gland has a variable shape and can be linear, inverted V or Y, triangular (Fig. 1) [25, 26]. One study found that normal adrenal limbs should be ≤3–5 mm [26].

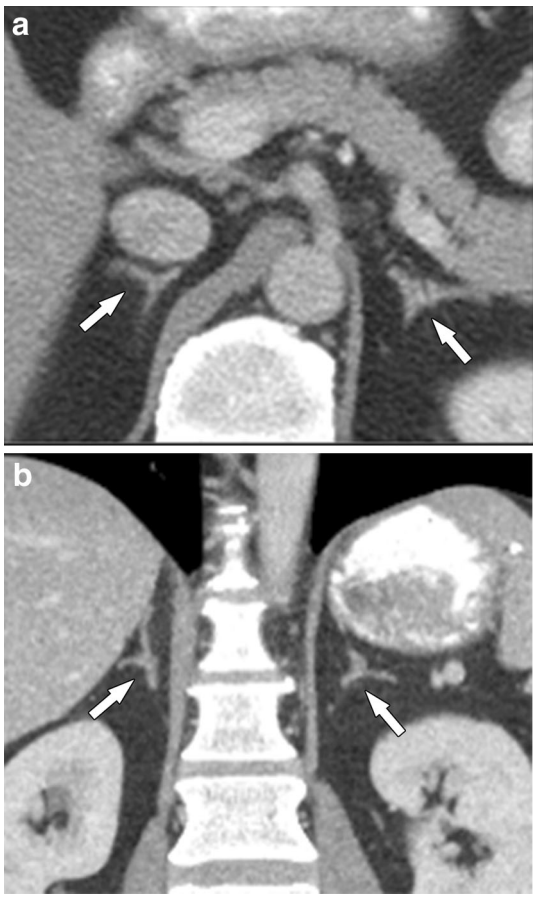

Fig. 1 Normal adrenal gland. **a** Contrast-enhanced axial CT scan image and **b** coronal reformatted image show the triangular shape of the adrenal glands (*arrows*) and its relationship to the diaphragm and kidneys

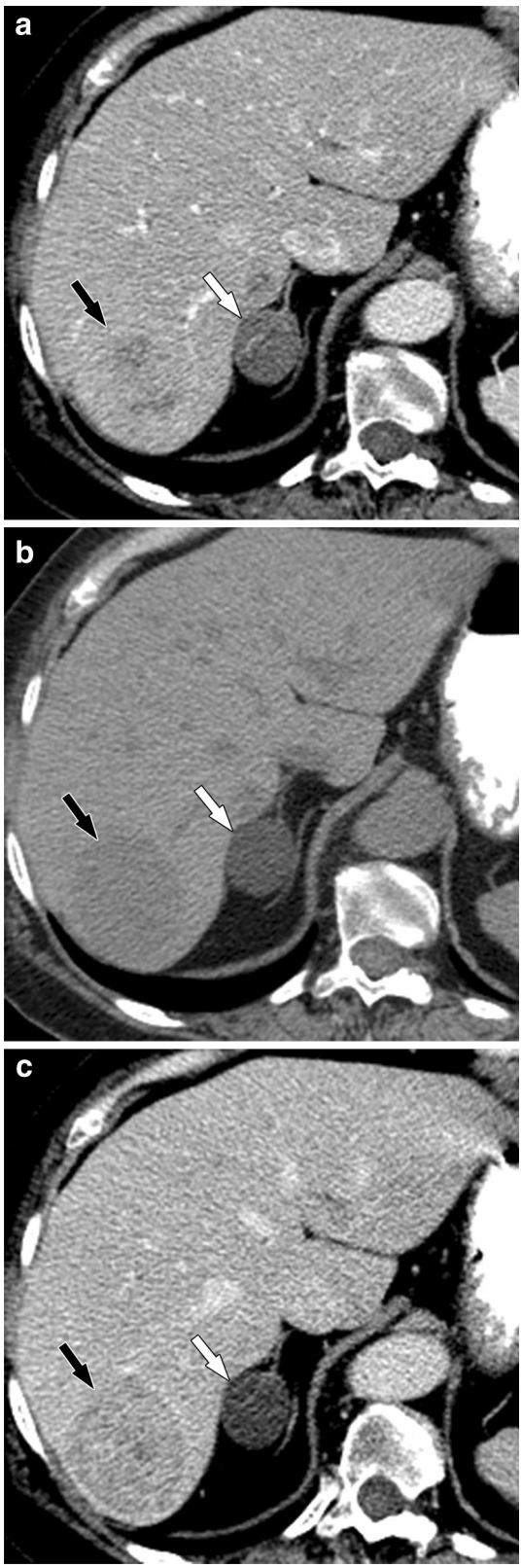

Fig. 2 Lipid-rich adrenal adenoma. **a** Pre-contrast-enhanced axial CT scan image demonstrates a well-defined round homogeneous lesion (*white arrows*) in the right adrenal gland. The pre-contrast attenuation measurement is −6 HU. **b** On the dynamic enhanced phase at 60 s after intravenous administration of contrast material, the attenuation measurement is 60 HU. **c** On the 15-min delayed image, the attenuation of the lesion is 18 HU. The calculated absolute contrast enhancement washout is 63 %, suggestive of a lipid-rich adenoma. Patient is a 66-year-old woman with hepatic metastases from small bowel neuroendocrine cancer (*black arrows*)

AdenomaAdenomas are the most prevalent adrenal lesion and have been detected in 2–9 % of autopsies. The frequency of adenomas is related to age, with these lesions occurring in approximately 0.14 % of 20- to 29-year-olds, and 7 % of persons older than 70 years old.

The size of adenomas ranges, with the majority measuring, 2–2.5 cm [27]. Rarely, adenomas are larger, measuring up to approximately 4–6 cm [4]. No definitive size criterion exists to definitively distinguish benign from malignant adrenal lesions. A study by Wajchenberg et al. found that adrenal lesions less than 3 cm are likely to be benign and lesions greater than 3 cm are likely to be malignant [28]. Typically, with no history of cancer, adrenal lesions smaller than 3 cm are likely to be benign. If an adrenal lesion is larger than 5 cm, surgical removal is advised [29].

Adenomas are usually well defined. The majority are homogeneous on noncontrast imaging. An important feature is the presence of intracellular lipid. The attenuation values depend on the amount of lipid. Lipid-rich adenomas range from −2 to 16 HU on noncontrast imaging (Fig. 2). Lipid-poor adenomas constitute about 10–40 % of adenomas, with higher attenuation on noncontrast imaging of 20–25 HU (Fig. 3) [25, 30]. Adenomas can be characterized by utilizing the washout calculations previously described. Irrespective of the lipid content, adenomas typically demonstrate rapid washout, with an absolute percentage washout (APW) of greater than 60 % and relative percentage washout (RPW) greater than 40 %. Occasionally adenomas can hemorrhage, as depicted by areas of increased attenuation and heterogeneity [29]. The differentiation between nonfunctioning and hyperfunctioning adenomas is a clinical diagnosis and cannot be made on CT imaging.

Hyperplasia

One study found that normal adrenal limbs should be ≤3–5 mm [26]. In adrenal hyperplasia, the medial and lateral limbs are larger and can present as smooth, nodular, or lobular. The CT attenuation is typically similar to that for a normal adrenal gland, with pre-contrast imaging lower in a few cases. In one study using a 3-mm cutoff, sensitivity for hyperplasia was 100 % and specificity was 54 % [31]. In that study using a 5-mm cutoff, sensitivity was 47 % and specificity was 100 % [31]. Hyperplasia can be caused by hormonal abnormalities, including Cushing's syndrome (hypercortisolism) and Conn's syndrome

Fig. 3 Lipid-poor adrenal adenoma. **a** Pre-contrast-enhanced axial CT scan image demonstrates a well-defined homogeneous round lesion in the left adrenal gland (*arrows*). The pre-contrast attenuation measurement is 16 HU. **b** On the dynamic enhanced phase at 60 s after intravenous administration of contrast material, the attenuation measurement is 76 HU. **c** On the 15-min delayed image, the attenuation of the lesion is 34 HU. The calculated absolute contrast enhancement washout is 70 %, suggestive of a lipid-poor adenoma. Patient is a 66-year-old man with melanoma

(hyperaldosteronism) (Fig. 4) [25, 31]. Identification of hyperplasia necessitates clinical evaluation, since it can be associated with hormonal abnormalities.

Fig. 4 Adrenal hyperplasia. Contrast-enhanced axial CT scan image demonstrates diffuse thickening of the limbs of the bilateral adrenal glands (*arrows*) in a 27-year-old man with Cushing syndrome

Myelolipoma

Myelolipomas are benign, typically incidental tumors composed of adipose tissue and hematopoietic tissue They commonly originate from the adrenal gland and rarely from an extra-adrenal location. Myelolipomas have been reported to range in size from 2 to 17 cm, with an average of 10 cm [6, 32, 33]. The CT presentation features a well-circumscribed lesion containing various amounts of soft tissue and fat (Fig. 5). The presence of macroscopic fat measuring −30 to −100 HU is characteristic of a myelolipoma. One study found that 50–90 % of myelolipomas contain fat, around 75 % have a pseudocapsule, and approximately 24 % have calcifications [34, 35].

A myelolipoma is a nonfunctional tumor and is typically asymptomatic. Symptoms can arise due to hemorrhage; in such cases patients can present with hypotension, pain, and vomiting (Fig. 6). A myelolipoma can also undergo necrosis or mass effect, also causing symptoms.

Adrenal Metastases

The most common malignant process involving the adrenal gland is metastasis. The adrenal gland is a common site of metastatic disease, preceded only by metastases of the lung, liver, and bone. In non-adrenal-related cancers, approximately 50–75 % of detected adrenal masses are metastases. Over 90 % of adrenal metastases in one study were from carcinomas, including lung, breast, colon, renal, pancreatic, esophageal, gastric, and hepatobiliary carcinomas [36, 37]. Approximately 56 % were adenocarcinomas, 15 % were squamous, and the remainder included melanomas, sarcomas, and hematopoietic tumors. In patients younger than 40 years old, common primary tumors with

Fig. 5 Myelolipoma. **a** Pre-contrast-enhanced axial CT scan image demonstrates a well-defined heterogeneous lesion containing soft tissue and macroscopic fat (*white arrows*). **b** Post-contrast-enhanced axial CT scan image and **c** coronal reformatted image show the origin of the mass (*white arrows*) from the right adrenal gland and compression of the right kidney inferiorly, suggestive of a myelolipoma. Patient is a 77-year-old man. Note the normal left adrenal gland (*black arrow*)

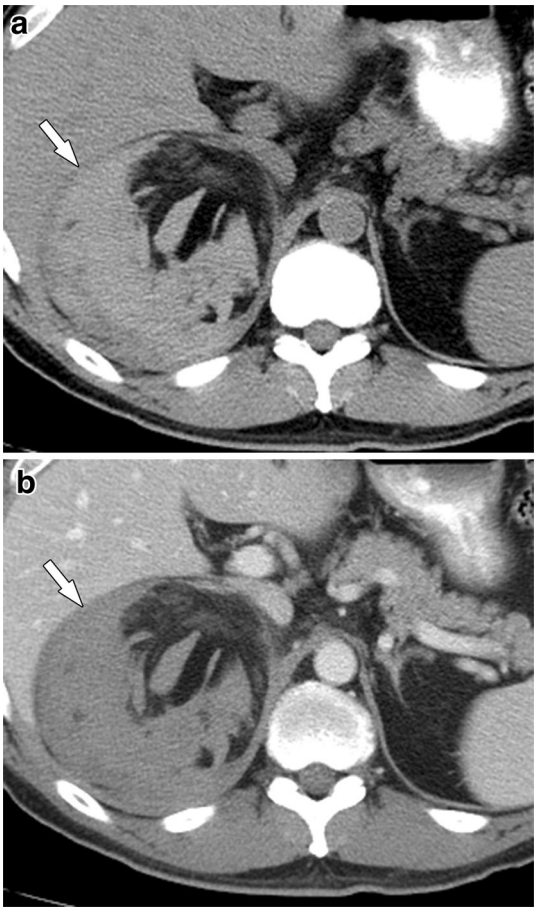

Fig. 6 Myelolipoma with hemorrhage. **a** Pre-contrast-enhanced axial CT scan image demonstrates a large heterogeneous fat lesion with high attenuation content (*arrows*), suggestive of hemorrhage. **b** Post-contrast-enhanced axial CT scan image shows the origin of the mass from the right adrenal gland displacing the inferior vena cava anteriorly, suggestive of a hemorrhagic myelolipoma. Patient is a 51-year-old man. Note the normal left adrenal gland (*black arrow*)

adrenal metastases include lung cancer, stomach cancer, and leukemia/lymphoma. One study reported that adrenal metastases are bilateral in 49 % of cases; when unilateral, metastases are more common on the left side [27, 38]. The CT presentation of metastases is variable. Hypervascular metastases, including those of renal cell carcinoma, can enhance avidly like pheochromocytomas. Typically metastases have noncontrast attenuation values >10 HU [7•]. A study by Blake et al. demonstrated that pre-contrast values range from 14 to 50 HU, with an average APW of 30.8 % and RPW of 15.3 % [39]. Metastases tend to have a slower washout pattern on delayed imaging, with an APW of <60 % and RPW of <40 %, in contrast to adenomas, which tend to have an APW of >60 %, and RPW of >40 % (Figs. 7, 8, 9, 10) [36, 40–42].

Adrenal Cortical Carcinoma

The prevalence of ACC is bimodal, with these tumors occurring during the 1st and 4th decades. Because the tumor is hormonally active, it is typically detected earlier.

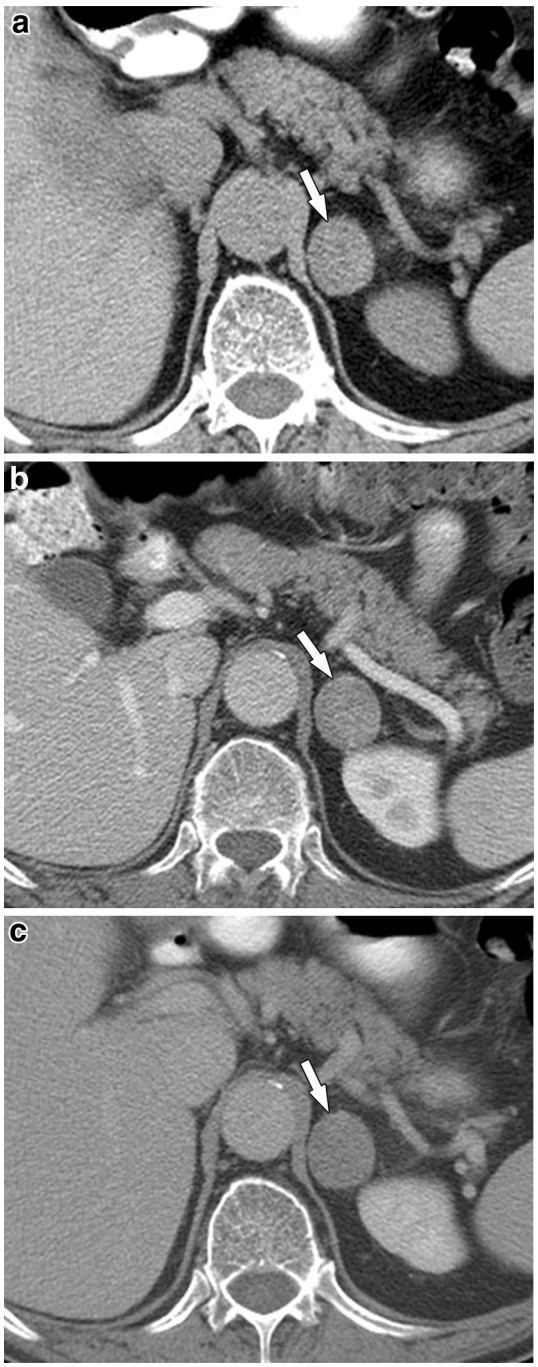

Fig. 7 Adrenal metastasis. **a** Pre-contrast-enhanced axial CT scan image demonstrates an enlarged lesion in the left adrenal gland (*arrows*), with attenuation of 35 HU. **b** Dynamic enhanced axial CT scan image obtained at the portal venous phase after intravenous administration of contrast material demonstrates an attenuation of 69 HU. **c** Delayed image demonstrates an attenuation of 55 HU. The calculated relative washout is 20 % in this 73-year-old man with melanoma suggestive of an adrenal gland metastatic lesion. Biopsy confirmed the diagnosis of metastasis

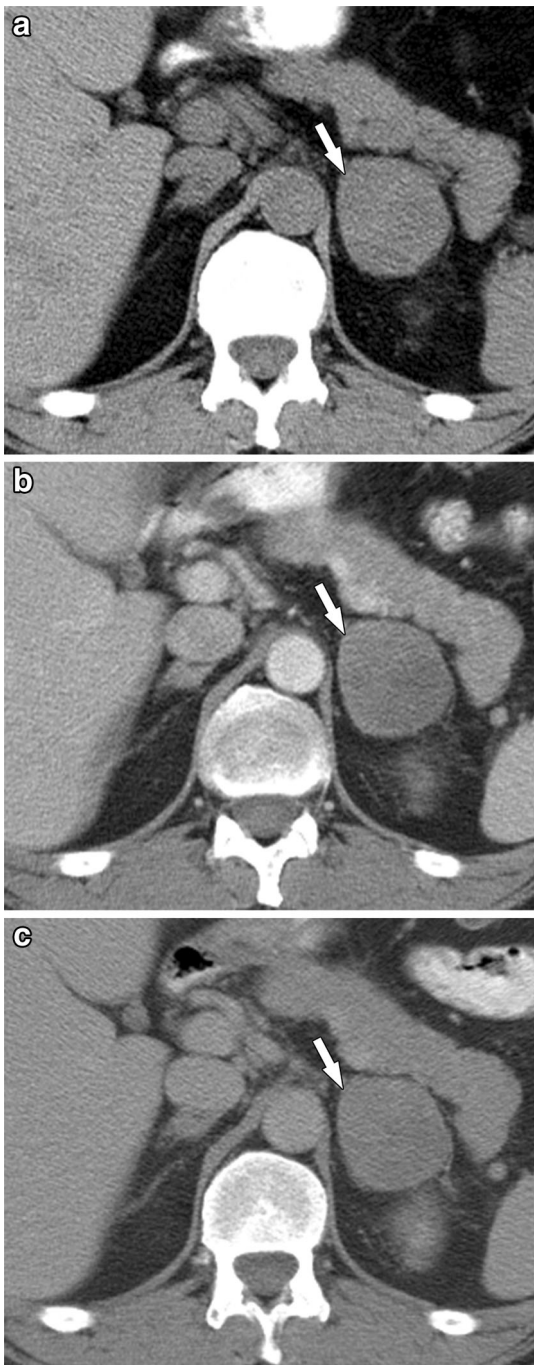

Fig. 8 Adrenal metastasis. **a** Pre-contrast-enhanced axial CT scan image demonstrates an enlarged lesion in the left adrenal gland (*arrows*), with attenuation of 30 HU. **b** Dynamic enhanced axial CT scan image obtained at 60 s after intravenous administration of contrast material demonstrates an attenuation of 38 HU. **c** Delayed image demonstrates persistent enhancement of the adrenal gland lesion, with an attenuation of 42 HU. There is no washout of contrast at the delayed images. These imaging findings are suggestive of an adrenal gland metastatic lesion. Patient is a 56-year-old man with melanoma. Biopsy confirmed the diagnosis of metastasis

Fig. 9 Adrenal metastasis. Contrast-enhanced axial CT scan images at baseline (**a**) and at 4 months after the diagnosis (**b**) demonstrating an interval increase in size of the metastatic lesions (*arrows*) in the bilateral adrenal glands of a 50-year-old man with non-small cell lung cancer. Biopsy confirmed the diagnosis of metastasis

Fig. 10 Adrenal metastasis. Contrast-enhanced axial CT scan image demonstrates avid enhancing lesions in the bilateral adrenal glands (*arrows*) in a 70-year-old woman with renal cell carcinoma, suggestive of bilateral metastatic lesions. Biopsy confirmed the diagnosis of metastasis

Patients may present with a palpable mass or abdominal symptoms. In approximately 55 % of ACCs (range of 26–94 %), symptoms of hypertension, feminization, virilization, or Cushing syndrome are detected [28]. ACCs are typically large masses, with a size range of 4–25 cm and the average being >6 cm. The degree of hormonal activity is typically inversely proportionate to tumor size [28, 43]. On noncontrast imaging, ACCs are typically heterogeneous, particularly larger tumors, due to the presence of necrosis. Calcifications, more commonly microcalcifications, have been identified in 19–33 % of cases in one study [44]. The tumors typically exhibit heterogeneous enhancement, occasionally with a thin-rim-enhancing capsule (Fig. 11). The degree of heterogeneity and larger size are more reliable features than the washout features. ACCs typically have an RPW of less than 40 %. Invasion of the inferior vena cava is a classic feature of advanced ACCs [29, 44, 45]. The most common metastatic site is the

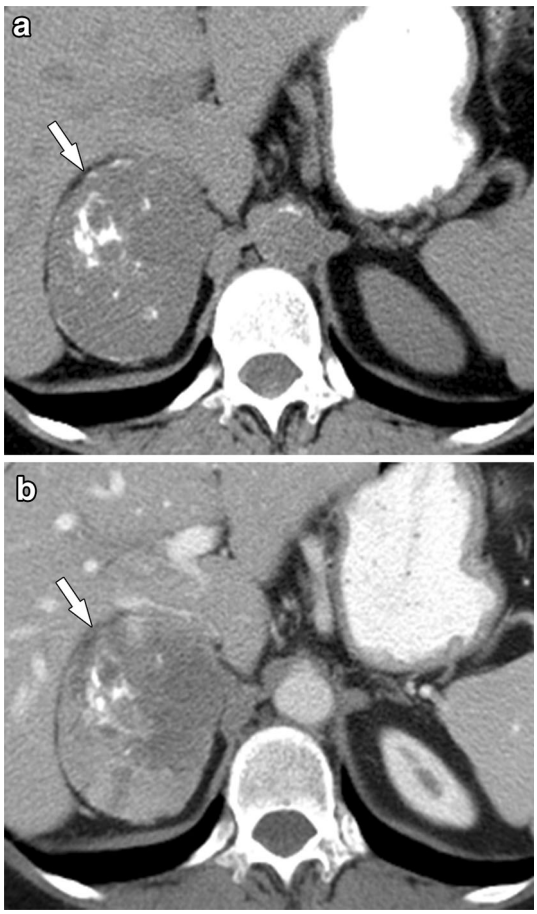

Fig. 11 Adrenal cortical carcinoma. **a** Pre-contrast-enhanced axial CT scan image demonstrates a large heterogeneous lesion with calcifications (*arrow*) originating from the right adrenal gland. **b** Contrast-enhanced axial CT scan image demonstrates the heterogeneous enhancement of the lesion (*arrow*), suggestive of an adrenal cortical carcinoma. Patient is a 67-year-old woman

Fig. 12 Pheochromocytoma. **a** Pre-contrast-enhanced axial CT scan image demonstrates a lesion in the right adrenal gland. Contrast-enhanced axial CT scan image at the arterial phase (**b**) and portal venous phase (**c**) shows intense enhancement of this lesion. **d** Contrast-enhanced axial CT scan obtained 15 min after the injection of contrast shows washout of the lesion in a 16-year-old man with von Hippel–Lindau disease. The pre-contrast, arterial phase, portal venous phase, and delayed attenuation measurements are 45, 160, 180, and 80 HU, respectively. The relative calculated washout is 55.6 %

liver; other sites of involvement include the lung and lymph nodes [44].

Pheochromocytoma

The prevalence of pheochromocytomas is 0.1–0.2 % in patients presenting with hypertension. A common symptom is new onset, paroxysmal, refractory, or recently exacerbated hypertension [46]. Pheochromocytoma has been shown to follow the rule of 10 s, with 10 % being malignant, bilateral, extra-adrenal, and familial [36]. Approximately 10 % of pheochromocytomas are asymptomatic. Patients with symptoms present with headache, flushing, and palpitations [27]. In 10 % of cases, pheochromocytomas can be associated with a variety of syndromes, including von Hippel-Lindau disease, neurofibromatosis, Sturge-Weber syndrome, tuberous sclerosis, and multiple endocrine neoplasia type 2 [46]. The diagnosis of pheochromocytoma can be made from laboratory tests. A 24-h vanillylmandelic acid, catecholamines, and metanephrines can be obtained. Plasma-free metanephrine levels can also be measured, typically when there is a high clinical suspicion for pheochromocytoma. The size of pheochromocytomas varies. They tend to be larger than adenomas, but not as large as metastases. The functional masses tend to be smaller than the nonfunctional ones. On CT, the classic presentation is strong enhancement [47]. A study demonstrated that nonionic intravenous contrast is safe for pheochromocytoma patients not taking alpha-blocker medications prior to the scan [48]. The contrast washout pattern can be variable. Pheochromocytomas can contain intracellular fat, calcification, and/or areas of cystic degeneration. Approximately 3–19 % of pheochromocytomas demonstrate fluid attenuation. The washout pattern may mimic a lipid-poor adenoma, with an APW of greater than 60 % and RPW greater than 40 %. A study by Patel et al. found that in 24 cases of pheochromocytomas, there was a 33 % overlap of enhancement patterns with lipid-poor adenomas, when using absolute and relative washout criteria with triphasic CT [49]. Dual-phase CT imaging has been used to differentiate pheochromocytomas from lipid-poor adenomas. A study by Northcutt et al. demonstrated that pheochromocytomas tend to have higher degrees of

enhancement in the arterial phase and tend to measure greater than 110 HU in the arterial phase. That study also demonstrated that pheochromocytomas tend to have heterogeneous features in comparison with adenomas. [50] In contrast, adenomas tend to have equivalent imaging across the arterial and venous phases or increased enhancement on venous imaging instead of arterial imaging [50]. Pheochromocytomas tend to have a greater percent washout than metastases (Fig. 12) [51, 52]. A study demonstrated that nonionic intravenous contrast is safe for pheochromocytoma patients not taking alpha-blocker medications prior to the scan.

Conclusion

Adrenal masses are commonly detected with the increased use of CT imaging for medical diagnoses. It is important for physicians to be familiar with the CT imaging techniques commonly used to characterize adrenal masses as well as the typical CT presentations of benign and malignant masses in order to avoid unnecessary work-up and to be able to determine which adrenal masses can be left alone and which need to be medically or surgically managed.

Compliance with Ethics Guidelines

Conflict of Interest Dr. Brinda Rao Korivi, Dr. Khaled M. Elsayes, Dr. Silvana Faria de Castro, Dr. Naveen Garg, and Dr. Aliya Qayyum each declare no potential conflicts of interest.

Human and Animal Rights and Informed Consent This article does not contain any studies with human or animal subjects performed by any of the authors.

References

Papers of particular interest, published recently, have beenhighlighted as:
- • Of importance
- •• Of major importance

1. Papierska L, Cichocki A, Sankowski AJ, Cwikla JB. Adrenal incidentaloma imaging—the first steps in therapeutic management. Pol J Radiol/Pol Med Soc Radiol. 2013;78(4):47–55.
2. Bovio S, Cataldi A, Reimondo G, Sperone P, Novello S, Berruti A, Borasio P, Fava C, Dogliotti L, Scagliotti GV, et al. Prevalence of adrenal incidentaloma in a contemporary computerized tomography series. J Endocrinol Invest. 2006;29(4):298–302.
3. Song JH, Chaudhry FS, Mayo-Smith WW. The incidental adrenal mass on CT: prevalence of adrenal disease in 1,049 consecutive adrenal masses in patients with no known malignancy. AJR Am J Roentgenol. 2008;190(5):1163–8.
4. Kloos RT, Gross MD, Francis IR, Korobkin M, Shapiro B. Incidentally discovered adrenal masses. Endocr Rev. 1995;16(4):460–84.
5. Hedeland H, Ostberg G, Hokfelt B. On the prevalence of adrenocortical adenomas in an autopsy material in relation to hypertension and diabetes. Acta medica Scandinavica. 1968;184(3):211–4.
6. Blake MA, Cronin CG, Boland GW. Adrenal imaging. AJR Am J Roentgenol. 2010;194(6):1450–60.
7. • Boland GW, Hahn PF, Pena C, Mueller PR. Adrenal masses: characterization with delayed contrast-enhanced CT. Radiology. 1997;202(3):693–6. *This study showed that adrenal masses can be characterized as benign or malignant on early delayed contrast-enhanced CT scans of the adrenal glands.*
8. Szolar DH, Kammerhuber FH. Adrenal adenomas and nonadenomas: assessment of washout at delayed contrast-enhanced CT. Radiology. 1998;207(2):369–75.
9. •• Caoili EM, Korobkin M, Francis IR, Cohan RH, Platt JF, Dunnick NR, Raghupathi KI. Adrenal masses: characterization with combined unenhanced and delayed enhanced CT. Radiology. 2002;222(3):629–33. *This study demonstrated that nearly all adrenal masses can be characterized as adenomas or nonadenomas based on combining use of noncontrast and delayed post-contrast CT imaging.*
10. Korivi BR, Elsayes KM. Cross-sectional imaging work-up of adrenal masses. World J Radiol. 2013;5(3):88–97.
11. Shi JW, Dai HZ, Shen L, Xu DF. Dual-energy CT: clinical application in differentiating an adrenal adenoma from a metastasis. Acta Radiol. 2014;55(4):505–12.
12. Gupta RT, Ho LM, Marin D, Boll DT, Barnhart HX, Nelson RC. Dual-energy CT for characterization of adrenal nodules: initial experience. AJR Am J Roentgenol. 2010;194(6):1479–83.
13. Ho LM, Marin D, Neville AM, Barnhart HX, Gupta RT, Paulson EK, Boll DT. Characterization of adrenal nodules with dual-energy CT: can virtual unenhanced attenuation values replace true unenhanced attenuation values? AJR Am J Roentgenol. 2012;198(4):840–5.
14. Gnannt R, Fischer M, Goetti R, Karlo C, Leschka S, Alkadhi H. Dual-energy CT for characterization of the incidental adrenal mass: preliminary observations. AJR Am J Roentgenol. 2012;198(1):138–44.
15. Helck A, Hummel N, Meinel FG, Johnson T, Nikolaou K, Graser A. Can single-phase dual-energy CT reliably identify adrenal adenomas? Eur Radiol. 2014;24(7):1636–42.
16. Kim YK, Park BK, Kim CK, Park SY. Adenoma characterization: adrenal protocol with dual-energy CT. Radiology. 2013;267(1):155–63.
17. Foti G, Faccioli N, Manfredi R, Mantovani W, Mucelli RP. Evaluation of relative wash-in ratio of adrenal lesions at early biphasic CT. AJR Am J Roentgenol. 2010;194(6):1484–91.
18. Foti G, Faccioli N, Mantovani W, Malleo G, Manfredi R, Mucelli RP. Incidental adrenal lesions: accuracy of quadriphasic contrast enhanced computed tomography in distinguishing adenomas from nonadenomas. Eur J Radiol. 2012;81(8):1742–50.
19. Qin HY, Sun HR, Li YJ, Shen BZ. Application of CT perfusion imaging to the histological differentiation of adrenal gland tumors. Eur J Radiol. 2012;81(3):502–7.
20. Bae KT, Fuangtharnthip P, Prasad SR, Joe BN, Heiken JP. Adrenal masses: CT characterization with histogram analysis method. Radiology. 2003;228(3):735–42.
21. Remer EM, Motta-Ramirez GA, Shepardson LB, Hamrahian AH, Herts BR. CT histogram analysis in pathologically proven adrenal masses. AJR Am J Roentgenol. 2006;187(1):191–6.
22. Jhaveri KS, Wong F, Ghai S, Haider MA. Comparison of CT histogram analysis and chemical shift MRI in the characterization

of indeterminate adrenal nodules. AJR Am J Roentgenol. 2006;187(5):1303–8.
23. Ho LM, Paulson EK, Brady MJ, Wong TZ, Schindera ST. Lipid-poor adenomas on unenhanced CT: does histogram analysis increase sensitivity compared with a mean attenuation threshold? AJR Am J Roentgenol. 2008;191(1):234–8.
24. Halefoglu AM, Bas N, Yasar A, Basak M. Differentiation of adrenal adenomas from nonadenomas using CT histogram analysis method: a prospective study. Eur J Radiol. 2010;73(3):643–51.
25. Johnson PT, Horton KM, Fishman EK. Adrenal imaging with MDCT: nonneoplastic disease. AJR Am J Roentgenol. 2009;193(4):1128–35.
26. Wilms G, Baert A, Marchal G, Goddeeris P. Computed tomography of the normal adrenal glands: correlative study with autopsy specimens. J Comput Assist Tomogr. 1979;3(4):467–9.
27. Johnson PT, Horton KM, Fishman EK. Adrenal mass imaging with multidetector CT: pathologic conditions, pearls, and pitfalls. Radiographics. 2009;29(5):1333–51.
28. Wajchenberg BL, Albergaria Pereira MA, Medonca BB, Latronico AC, Campos Carneiro P, Alves VA, Zerbini MC, Liberman B, Carlos Gomes G, Kirschner MA. Adrenocortical carcinoma: clinical and laboratory observations. Cancer. 2000;88(4):711–36.
29. Johnson PT, Horton KM, Fishman EK. Adrenal imaging with multidetector CT: evidence-based protocol optimization and interpretative practice. Radiographics. 2009;29(5):1319–31.
30. Park SH, Kim MJ, Kim JH, Lim JS, Kim KW. Differentiation of adrenal adenoma and nonadenoma in unenhanced CT: new optimal threshold value and the usefulness of size criteria for differentiation. Korean J Radiol. 2007;8(4):328–35.
31. Lingam RK, Sohaib SA, Vlahos I, Rockall AG, Isidori AM, Monson JP, Grossman A, Reznek RH. CT of primary hyperaldosteronism (Conn's syndrome): the value of measuring the adrenal gland. AJR Am J Roentgenol. 2003;181(3):843–9.
32. Young WF Jr. Clinical practice. The incidentally discovered adrenal mass. N Engl J Med. 2007;356(6):601–10.
33. Russell C, Goodacre BW, vanSonnenberg E, Orihuela E. Spontaneous rupture of adrenal myelolipoma: spiral CT appearance. Abdom Imaging. 2000;25(4):431–4.
34. Kenney PJ, Wagner BJ, Rao P, Heffess CS. Myelolipoma: CT and pathologic features. Radiology. 1998;208(1):87–95.
35. Guo YK, Yang ZG, Li Y, Deng YP, Ma ES, Min PQ, Zhang XC. Uncommon adrenal masses: CT and MRI features with histopathologic correlation. Eur J Radiol. 2007;62(3):359–70.
36. Taffel M, Haji-Momenian S, Nikolaidis P, Miller FH: Adrenal imaging: a comprehensive review. Radiol Clin N Am. 2012;50(2):219–43, v.
37. Korobkin M. Overview of adrenal imaging/adrenal CT. Urol Radiol. 1989;11(4):221–6.
38. Lam KY, Lo CY. Metastatic tumours of the adrenal glands: a 30-year experience in a teaching hospital. Clin Endocrinol. 2002;56(1):95–101.
39. Blake MA, Kalra MK, Sweeney AT, Lucey BC, Maher MM, Sahani DV, Halpern EF, Mueller PR, Hahn PF, Boland GW. Distinguishing benign from malignant adrenal masses: multidetector row CT protocol with 10-min delay. Radiology. 2006;238(2):578–85.
40. Lenert JT, Barnett CC Jr, Kudelka AP, Sellin RV, Gagel RF, Prieto VG, Skibber JM, Ross MI, Pisters PW, Curley SA, et al. Evaluation and surgical resection of adrenal masses in patients with a history of extra-adrenal malignancy. Surgery. 2001;130(6):1060–7.
41. Gillams A, Roberts CM, Shaw P, Spiro SG, Goldstraw P. The value of CT scanning and percutaneous fine needle aspiration of adrenal masses in biopsy-proven lung cancer. Clin Radiol. 1992;46(1):18–22.
42. Abrams HL, Spiro R, Goldstein N. Metastases in carcinoma; analysis of 1,000 autopsied cases. Cancer. 1950;3(1):74–85.
43. Ng L, Libertino JM. Adrenocortical carcinoma: diagnosis, evaluation and treatment. J Urol. 2003;169(1):5–11.
44. Fishman EK, Deutch BM, Hartman DS, Goldman SM, Zerhouni EA, Siegelman SS. Primary adrenocortical carcinoma: CT evaluation with clinical correlation. AJR Am J Roentgenol. 1987;148(3):531–5.
45. Chiche L, Dousset B, Kieffer E, Chapuis Y. Adrenocortical carcinoma extending into the inferior vena cava: presentation of a 15-patient series and review of the literature. Surgery. 2006;139(1):15–27.
46. Mittendorf EA, Evans DB, Lee JE, Perrier ND: Pheochromocytoma: advances in genetics, diagnosis, localization, and treatment. Hematol/Oncol Clin N Am. 2007;21(3):509–25; ix.
47. Szolar DH, Korobkin M, Reittner P, Berghold A, Bauernhofer T, Trummer H, Schoellnast H, Preidler KW, Samonigg H. Adrenocortical carcinomas and adrenal pheochromocytomas: mass and enhancement loss evaluation at delayed contrast-enhanced CT. Radiology. 2005;234(2):479–85.
48. Bessell-Browne R, O'Malley ME. CT of pheochromocytoma and paraganglioma: risk of adverse events with i.v. administration of nonionic contrast material. AJR Am J Roentgenol. 2007;188(4):970–4.
49. Patel J, Davenport MS, Cohan RH, Caoili EM. Can established CT attenuation and washout criteria for adrenal adenoma accurately exclude pheochromocytoma? AJR Am J Roentgenol. 2013;201(1):122–7.
50. Northcutt BG, Raman SP, Long C, Oshmyansky AR, Siegelman SS, Fishman EK, Johnson PT. MDCT of adrenal masses: can dual-phase enhancement patterns be used to differentiate adenoma and pheochromocytoma? AJR Am J Roentgenol. 2013;201(4):834–9.
51. Motta-Ramirez GA, Remer EM, Herts BR, Gill IS, Hamrahian AH. Comparison of CT findings in symptomatic and incidentally discovered pheochromocytomas. AJR Am J Roentgenol. 2005;185(3):684–8.
52. Park BK, Kim CK, Kwon GY, Kim JH. Re-evaluation of pheochromocytomas on delayed contrast-enhanced CT: washout enhancement and other imaging features. Eur Radiol. 2007;17(11):2804–9.